X Workshop em Engenharia e Tecnologia Espaciais
7 a 9 de agosto de 2019

Numerical Modeling of a Heat Pipe Transient Modes

ENKE, C. [1], VLASSOV, V.[2]

[1]Instituto Nacional de Pesquisas Espaciais, São José dos Campos, SP, Brasil

Aluno de Mestrado do curso de Mecânica Espacial e Controle - CMC.

[2]Instituto Nacional de Pesquisas Espaciais, São José dos Campos, SP, Brasil

cristiano.enke@inpe.br

Resumo. *A transient one-dimensional mathematical model for a conventional heat pipe is presented and solved numerically. The model was developed using the energy conservation equation to simulate the temperature profile across the heat pipe shell, with source term account for the heat input and output from the pipe. Navier-Stokes equations were used to model the vapor flow considering the evaporation/condensation rates and compressible flow. The predictions of the model were compared with published experimental data for a copper-water heat pipe.*

Keywords: Heat Pipe; Numerical Modeling; Navier-Stokes Equation.

1. Introduction

A heat pipe is a device used to transport heat between two interfaces with high efficiency. The principle of heat pipe was conceived by [GAUGLER, 1944], but its applications and effectiveness was showed by Grover and his colleagues from Los Alamos Scientific Laboratory [GROVER et al. 1964].

In its conventional and simplest form, a heat pipe is composed by a closed tube with its inner surfaces lined with a porous material or capillary wick. The wick structure is saturated with liquid and the remaining volume contains the vapor phase of a working fluid. When a heat load is applied at some section of the heat pipe by an external source, this heat vaporizes the working fluid at that. This additional vapor generated results in a difference in pressure at the core of the pipe driving vapor from evaporator to the condenser zone where the vapor condenses and releases the latent heat of vaporization to a heat sink. When liquid is depleted by evaporation at evaporator zone, a capillary pressure is developed there. This capillary pressure pumps the condensed liquid back from condenser to evaporator. This dynamics can be seen in Figure 1.1.

The problem of mathematically solve the behavior of heat pipes was already faced by many investigators. [BOWMAN, 1987] presented a two-dimensional model of steady compressible vapor dynamics of a heat pipe. [ISSACCI et al, 1989] presented a two-dimensional transient model of vapor dynamics of a rectangular cross section heat pipe. [FAGHRI, 1991] and his colleagues, in a series of reports [JANG et al., 1989a; JANG et

al., 1989b] presented a transient model to simulate the startup from frozen state of high temperature heat pipes, in which a one-dimensional approach is used to account the vapor dynamics and those equations were coupled with a two-dimensional mesh for wall and wick structure. [HALL and DOSTER, 1990] presented the code THROHPUT, capable to simulate a transient two-dimensional model of high temperature heat pipes from frozen state, and allows the presence of noncondensable gas within vapor. And [TOURNIER and EL-GENK, 1996] presented the code HPTAM to simulate a transient two-dimensional model of heat pipes from frozen state with the presence of noncondensable gas within vapor and the liquid flow inside the wick.

The objective of this study is to present a mathematical model of transient behavior of a conventional heat pipe during startup and solve the equations numerically. The model should be able to predict the temperatures at wall and vapor, the vapor pressure and velocities as well as densities and vapor mass flux at the core.

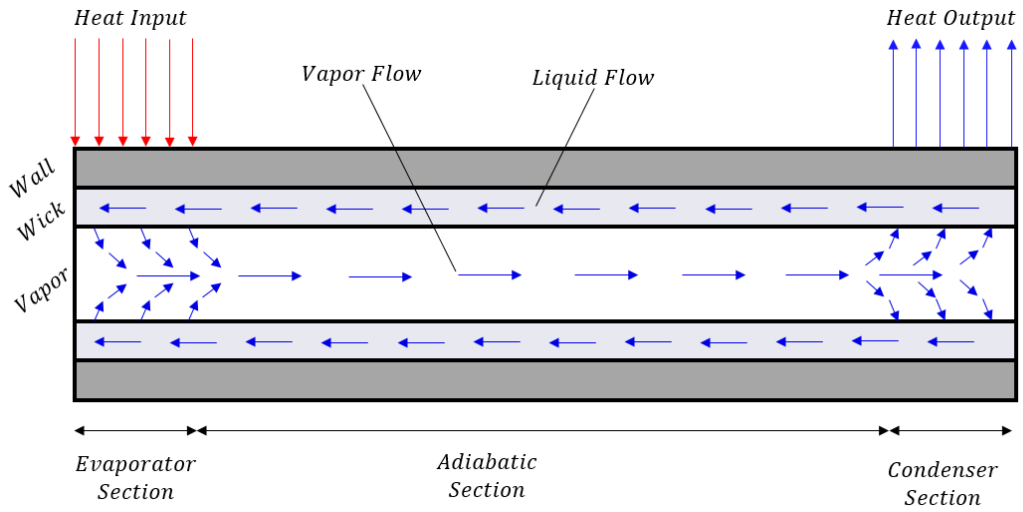

Figure 1.1 - Schematics and principles of operation of a conventional Heat Pipe.

Nomenclature:

C_p = specific heat at constant pressure, J/kgK

D_v = vapor channel diameter, m

f = friction coefficient

h_x = convection coefficient between wall and wick regions, W/m^2K

h_{x2} = convection coefficient between the wick region and vapor, W/m^2K

h_{amb} = convection coefficient between wall

Q_{in} = volumetric rate of heat input from heat source, W/m^3

R_v = gas constant of fluid, J/kgK

Re = Reynolds Number

t = time, s

T_{amb} = ambient temperature and, K

T_{stag} = stagnation temperature, K

T_{vap} = vapor temperature, K

T_{wall} = wall temperature, K

and ambient, W/m^2K
j = mass flux, kg/m^2s
k = thermal conductivity of wall, W/mK
k_{eff} = effective thermal conduction of the wick structure, W/mK
p = pressure, Pa
p_{stag} = stagnation pressure, Pa
q = heat flux, W/m^2
T_{wick} = temperature of wick region, K
u = vapor velocity, m/s
w = separation between grooves, m
z = coordinate along the axis, m

Greek Symbols:
ε = wick porosity
λ = latent heat of evaporation, J/kg
ρ = vapor density, kg/m^3
μ = dynamic viscosity, $Pa\,s$

2. Mathematical and Numerical Modeling

The continuity equation, for a compressible fluid with mass source, as presented by [JANG et al., 1989a] is the following:

$$\frac{\partial \rho}{\partial t}+\frac{\partial \rho u}{\partial z}=\frac{4j}{D_v}, \tag{2.1}$$

The momentum equation of vapor, as presented by [JANG et al., 1989a]:

$$\frac{\partial \rho u}{\partial t}+\frac{\partial \rho u u}{\partial z}=-\frac{\partial p}{\partial z}+\frac{4}{3}\mu\frac{\partial^2 u}{\partial z^2}-\frac{\rho u^2 f}{D_v}, \tag{2.2}$$

Considering a circular heat pipe with vapor flow always laminar, the friction factor is:

$$f=\frac{16}{\mathrm{Re}}, \tag{2.3}$$

Under the assumption that the vapor flow is compressible and laminar, the momentum equation gets the format as follows,

$$\rho\frac{\partial u}{\partial t}+u\frac{\partial \rho u}{\partial z}+\rho u\frac{\partial u}{\partial z}=-\frac{\partial p}{\partial z}+\frac{4}{3}\mu\frac{\partial^2 u}{\partial z^2}-\frac{32\mu u}{D_v^2}. \tag{2.4}$$

The heat equation at the wall, with source term, adapted from [JANG et al, 1989b]:

$$\rho C_p\frac{\partial T_{wall}}{\partial t}=k\frac{\partial^2 T_{wall}}{\partial z^2}+Q_{in}+\frac{h_x}{\delta}\left(T_{wick}-T_{wall}\right)+\frac{h_{amb}}{\delta}\left(T_{amb}-T_{wall}\right), \tag{2.5}$$

The heat equation of the wick structure was adapted from [FAGHRI,1991] and [DAS et al., 2017], considering incompressible liquid flow, no viscous dissipation, neglecting the velocity of liquid to the heat transfer coefficient, and considering heat exchange with vapor core and heat pipe wall:

$$\left(\rho C_p\right)\frac{\partial T_{wick}}{\partial t}=k_{eff}\frac{\partial^2 T_{wick}}{\partial z^2}+\frac{h_{x2}}{\delta}\left(T_{vap}-T_{wick}\right)+\frac{h_x}{\delta}\left(T_{wall}-T_{wick}\right), \tag{2.6}$$

in this equation the volumetric specific heat $\left(\rho C_p\right)$ is defined by:

$$\left(\rho C_p\right)=\left(\varepsilon\left(\rho C_p\right)_l+\left(1-\varepsilon\right)\left(\rho C_p\right)_s\right), \tag{2.7}$$

and k_{eff} for porous structures is:

$$k_{eff}=\varepsilon k_l+\left(1-\varepsilon\right)k_s, \tag{2.8}$$

and for grooved structures with grooves evenly spaced:

$$k_{eff}=\frac{wk_l+wk_s}{2w}. \tag{2.9}$$

The energy equation of vapor from [JANG et al., 1989b] solved directly for temperature:

$$C_p\frac{\partial\rho T_{vap}}{\partial t}+C_p\frac{\partial\rho uT_{vap}}{\partial z}=k\frac{\partial^2T_{vap}}{\partial z^2}+u\frac{\partial p}{\partial z}+\frac{4}{3}\mu\frac{\partial^2u}{\partial z^2}+\frac{4}{3}\mu\left(\frac{\partial u}{\partial z}\right)^2+\frac{4jC_pT_{vap}}{D_v}-\frac{2\rho u^3f}{D_v}, \tag{2.10}$$

and considering laminar flow it becomes,

$$C_p\frac{\partial\rho T_{vap}}{\partial t}+C_p\frac{\partial\rho uT_{vap}}{\partial z}=k\frac{\partial^2T_{vap}}{\partial z^2}+u\frac{\partial p}{\partial z}+\frac{4}{3}\mu\frac{\partial^2u}{\partial z^2}+\frac{4}{3}\mu\left(\frac{\partial u}{\partial z}\right)^2+\frac{4jC_pT_{vap}}{D_v}-\frac{32\mu u^2}{D_v^2}, \tag{2.11}$$

The equation of evaporation/condensation mass rate:

$$j=\frac{q}{\lambda}=\frac{h_{x2}}{\lambda}\left(T_{wick}-T_{vap}\right), \tag{2.12}$$

The Equation 4.16 takes into account that all heat added to vapor will cause evaporation and all heat removed from vapor will cause condensation, that is because it is considered that the fluid is in its saturation state, which causes that all heat added or removed responsible for phase change.

The Clausius-Clapeyron equation relates the temperature and pressure of a saturated fluid:

$$\ln\left(\frac{p}{p_{stag}}\right)=\frac{\lambda}{R_v}\left(\frac{1}{T_{stag}}-\frac{1}{T}\right), \tag{2.13}$$

The equation of state is used for vapor to link to its density:

$$p=\rho R_vT_v, \tag{2.15}$$

A staggered grid was used for the spatial discretization, so that the velocities are obtained in the faces and the other variables are obtained in the center of the control volumes. The numeric method SIMPLE, presented by [PATANKAR, 1980] was used to solve the pressure-velocity coupling. The discretization of the differential equations here presented resulted in algebraic systems of equations that were solved using the Thomas algorithm [ANDERSON, 1995], or TDMA (Tridiagonal Matrix Algorithm).

The numerical procedure is as follows:

1 - Input parameters, fluid and material properties.

2 - Input initial conditions of temperature, pressure, density and velocity.

3 - Input boundary conditions.

4 - Solve momentum equation with SIMPLE.

5 - Solve heat equation for wall and wick region.

6 - Calculate mass flux of evaporation/condensation.

7 - Solve energy equation.

8 - Calculate pressure with Clausius-Clapeyron equation.

9 - Calculate density with equation of state.

10 - Do an increment in time and all variables become the initial condition of next time step.

11 - Repeat steps 4-10 until final time step.

At the starting conditions with $t = 0$, all temperatures were considered in equilibrium with ambient and all velocities and fluxes are zero:

$$T_{wall}(0,z) = T_{amb}, \quad T_{wick}(0,z) = T_{amb}, \quad T_{vap}(0,z) = T_{amb}, \tag{2.16}$$

$$u(0,z) = 0, \quad j(0,z) = 0. \tag{2.19}$$

The starting pressure is the saturation pressure at T_{amb}:

$$p(0,z) = p_{stag} e^{\frac{\lambda}{R_v}\left(\frac{1}{T_{stag}} - \frac{1}{T_{vap}}\right)}. \tag{2.21}$$

And the density comes from the state equation:

$$\rho(0,z) = \frac{p(0,z)}{R_v T_{vap}(0,z)}. \tag{2.22}$$

At boundaries, a Neumann boundary condition was applied to the temperatures:

$$\frac{\partial T_{wall}(t,0)}{\partial z} = \frac{\partial T_{wall}(t,L)}{\partial z} = 0, \tag{2.23}$$

$$\frac{\partial T_{wick}(t,0)}{\partial z} = \frac{\partial T_{wick}(t,L)}{\partial z} = 0, \tag{2.24}$$

$$\frac{\partial T_{vap}(t,0)}{\partial z} = \frac{\partial T_{vap}(t,L)}{\partial z} = 0. \tag{2.25}$$

And no-slip condition to the vapor velocity:

$$u(t,0) = u(t,L) = 0. \tag{2.26}$$

3. Results and Discussion

To verify the model, a comparison with experimental data obtained by [FAGHRI and BUCHKO, 1991] was performed. A heat pipe made of copper has a length of 1m. The heat pipe shell is 1.7 mm, and the wick is 0.7 mm thick. The vapor core diameter has 20.5 mm. The working fluid considered is water. The heat pipe was modeled with 50 nodes. A total power input of 97 W was applied on nodes 3 to 5, corresponding the length of evaporator with 6.35 cm. Forced convection was applied on nodes 36 to 50, corresponding to the condenser length of 30 cm. Adiabatic conditions were considered for the rest of the nodes. Ambient temperature is 25 ºC.

The simulation was time-dependent, so an elapsed time of 2000 s, (with a time step of 1x10E-5) from startup was considered enough to stabilization and allows the comparison of the numerical results with a steady-state heat pipe experiment from literature

The entire simulation of 2000 s took approximately 77 minutes using a computer with an i5 processor with 2.5 GHz and 4 GB of RAM (Random Access Memory) in a 64 bits Operational System and a routine written in FORTRAN.

In Figure 3.1a is presented the temperature outer wall of the pipe, and in Figure 3.1b is presented the temperature of the vapor, both at first node of numeric model versus time. It is possible to see that after about 1400 s the system reached steady-state. The simulation was left running for more time to check for stability of the algorithm after long periods, but there were no divergence between the times analyzed.

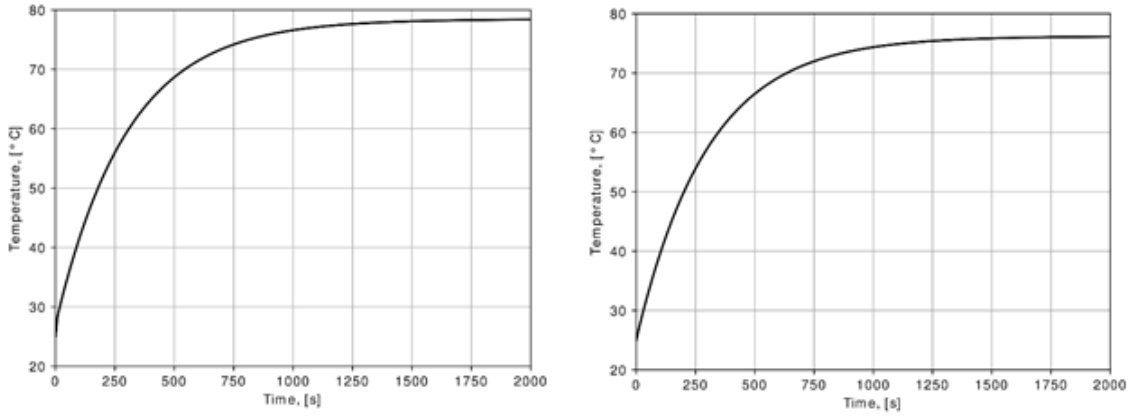

Figure 3.1 – (a)Temperature of the outer wall versus time and the (b) temperature of vapor versus time, both on the first node of model.

Figure 3.2 show the temperatures of the wall and vapor and the comparison between the numeric model and experimental data from [FAGHRI and BUCHKO, 1991]. A good agreement of the numeric model and experiment was achieved. As expected, a peak in temperature of wall occur at evaporator while the temperature falls at condenser, and the temperatures of vapor remains almost constant along pipe due to phase change.

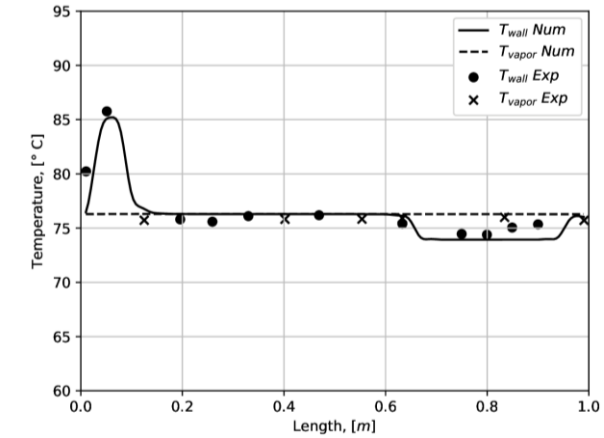

Figure 3.2 – Temperature of the outer wall and temperature of vapor with a comparison between numeric model and experimental data from [FAGHRI and BUCHKO, 1991].

In Figure 3.3 the velocities of vapor along the axis of the pipe is showed. It is possible to see a rise in the vapor velocity when it crosses the evaporator section, starting from zero at the end cap of the tube. While the vapor passes through the adiabatic zone, almost no energy is exchanged between vapor and wick structure, which causes the velocity remain constant in this section. At condenser, the vapor loses energy and velocity through the section until it reaches zero velocity at the other end cap of the tube.

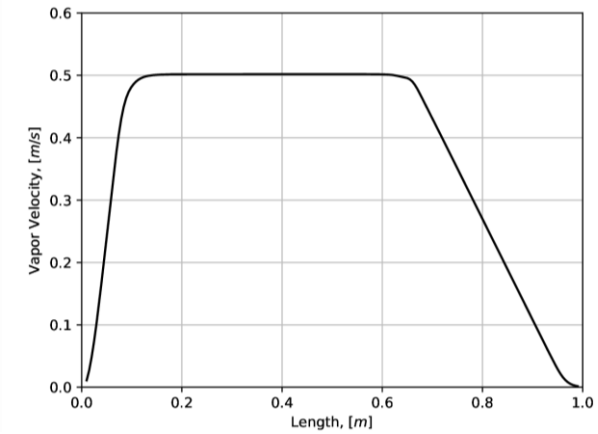

Figure 3.3 – Velocities of the vapor versus axial location.

At last, in Figure 3.4 is showed the mass flux of evaporation/condensation of vapor along the axis of the pipe. It is possible to see a profile very similar to the wall temperature, which was already expected. At evaporator, with higher temperatures, evaporation occurs and at condenser, with lower temperatures it is possible to see condensation occurring, while at adiabatic zone, almost no net flux of mass is visible.

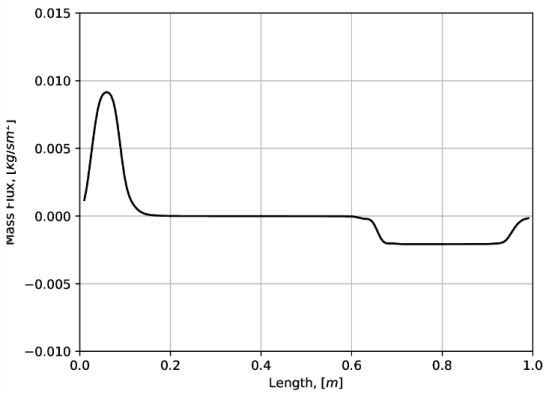

Figure 3.4 – Mass flux of evaporation/condensation versus axial location.

4. Conclusion

A one-dimensional model of the transient startup behavior of a conventional copper-water heat pipe was presented. The model allows a better understanding of the dynamics involving the startup process. The steady state part of the model shows a good agreement with steady-state experimental data from literature. The solution presented can be easily modified to represent multiples sources of heat or sinks and simulate any transient mode.

Acknowledgement: *Thanks to the Coordination of Improvement of Higher Education Personnel (CAPES).*

References

Anderson, J. D. (1995), Computational Fluid Dynamics: The Basics with Applications. Singapore: McGraw-Hill Education. 574 p.

Das, M. K.; Mukherjee, P. P.; Muralidhar, M. (2017), Modeling Transport Phenomena in Porous Media with Applications. Springer. 250 p.

Faghri, A. (1991), Analysis of Frozen Startup of High-Temperature Heat Pipes and Three-Dimensional Modeling of Block Heated Heat Pipes. Ohio. 138 p. Report Number WL-TR-91-2086

Faghri, A.; Buchko, M. (1991), Experimental and Numerical Analysis of Low-Temperature Heat Pipes With Multiple Heat Sources. Journal of Heat Transfer. v. 113, p. 728-734.

Gaugler, R. (1944), Heat Transfer Devices, US Patent number 2350348.

Grover, G. M.; Cotter, T. P.; Erikson, F. G. (1964), Structures of Very High Thermal Conductivity. Journal of Applied Physics. v. 35, p.

Jang, J. H.; Chang, W. S.; Faghri, A. (1989), Analysis of Transient Compressible Vapor Flow in Heat Pipe. Ohio. 10 p. NASA Contract Report 185119.

Jang, J. H.; Chang, W. S.; Mahefkey, E. T.; Faghri, A. (1989), Mathematical Modeling and Analysis of Heat Pipe Startup From Frozen State. Ohio. 12 p. NASA Contract Report 185132.

Patankar, S. V. (1980), Numerical Heat Transfer and Fluid Flow. England: CRC Press. 214 p.